 doi:10.20944/preprints202002.0280.v1

Novel morphological alteration and neural pathway of NADPH diaphorase positivity in the spinal cord with disc herniation of aged dog: A case report

Yinhua Li[1,3#], Yunge Jia[1, 2#], Wei Hou[1#], Huibing Tan[1,4*]

[1] Department of Anatomy, Jinzhou Medical University, Jinzhou, Liaoning 121001, China
[2] Department of Pathology, Heji Hospital Affiliated to Changzhi Medical College, Changzhi, Shanxi, 046011, China.
[3] School of Rehabilitation and Sports Medicine, Jinzhou Medical University, 121001, China
[4] Key Laboratory of Neurodegenerative Diseases of Liaoning Province, Jinzhou Medical University, Jinzhou, Liaoning, 121001, China

Running title: Lumbosacral neurodegeneration in spinal disc herniation of aged dog

*** Correspondence:**
Department of Anatomy, Jinzhou Medical University, Jinzhou, Liaoning 121001, China, davidtanhb@foxmail.com

# The first three authors make equal contributions to this work.

ABSTRACT

Neuronal lesion or injury is a traditional approach to investigate neural circuit. Is any new neural pathway or new neurodegeneration related central nerve system injury? Spinal disc herniation can cause the spinal cord injury. However, the histological examination is still lack. It happened that a case of spinal disc herniation of a 10-year old dog was examined with NADPH diaphorase (N-d) histology. We did not find the N-d neurodegenerative aberrant in the tissue of the mid-rostral lumber segment besides the metamorphoses by the compression of the disc herniation. However, the severe neuropathological changes majorly occurred in the lumbosacral spinal cord. We found more diverse neurodegenerative alterations: the aging-related N-d body (ANB), megaloneurite and N-d homogeneous formazan globule in the lumbosacral spinal cord. We also found that a new circuit pathway (intermedial collateral pathway) showed by a megaloneurite between the lateral collateral pathway and the medial collateral pathway. The enormous notch caused by spinal disc herniation located at the mid-rostral lumber segments. The aging-related neurodegeneration occurred the specific lumbosacral segments. The homogeneous formazan globule was round or oval homogeneous N-d positivity which distributed in the gray matter and dorsal column. In the medulla oblongata, ANBs were revealed in the gracile nucleus, nucleus reticularis lateralis (ventrolateral spinal trigeminal nucleus) and middle of the spinal trigeminal nucleus.

KEY WORDS: spinal disc herniation, dog, NADPH diaphorase, the aging-related NADPH diaphorase body, megaloneurite, homogeneous formazan globule, intermedial collateral pathway

Preprints (www.preprints.org) | NOT PEER-REVIEWED | Posted: 19 February 2020 doi:10.20944/preprints202002.0280.v1

INTRODUCTION

Thoracolumbar intervertebral disc herniations are a common disease that cause spinal cord injury (SCI) [1-5]. Cerebrospinal fluid (CSF) tau protein is found to be used as a biomarker in severity of SCI in dogs with intervertebral disc herniation [6]. Spinal cord swelling is used as indication for prognosis in intervertebral disc disease of dogs[7]. An experimental model of epidural balloon compression is found to cause the spinal cord occlusion and severe hemorrhages as well as vacuolar formations[8]. However, the neuropathological changes of intervertebral disc herniations are scarcely reported. We have found a megaloneurites of NADPH diaphorase (N-d) in the sacral spinal cord of the aged dogs[9] and aged monkey[10]. Recently, a case of 10-year old dog of lumber disc herniations happened to be investigated with N-d staining. Besides the occurrence of N-d megaloneurites in the sacral spinal cord, we further found the aging-related N-d body (ANB) and round or oval homogeneous N-d positivity in the spinal cord with disc herniations. Homogeneous formazan globule was a new term that we will discuses in the discussion section.

MATERIALS AND METHODS

The tissue preparation

Adult female dog (crossbreed dog Pekingese, 7.2kg) was legally obtained from Jinzhou Animal Facility for Department of Surgery (Jinzhou, China) and was breeding maintained in a temperature and humidity-controlled room as well as fed libitum. This study and experimental protocol were approved by the Ethics Committee on the Use of Animals at Jinzhou Medical University.

The animal was deeply anesthetized by intravenous injection of sodium pentobarbital (60 mg/kg body weight) and perfused through the aorta with physiological saline, followed by 4% paraformaldehyde in 0.1 M phosphate buffer (PB; pH 7.4) briefly according to the previous experiments[11]. The tissues of the brain and spinal cord were immersed in the same fixative as in the perfusion for 6 hrs. at 4°C, and transferred to 30% sucrose in 0.1 M PB (pH 7.4). Frozen sections were cut coronally at 40 μm on a cryostat.

NADPH diaphorase histochemistry

N-d enzyme histochemistry was performed in free-floating approach. In this procedure,

Sections were incubated for 5 min in 100 mM sodium phosphate buffer(PBS, pH 7.4) followed by incubation in phosphate buffer (PB, pH 7.4) with 1 mM beta-NADPH, 0.5 mM NBT and 0.3% Triton X-100 at 37℃ for up to 3h. Sections were rinsed with PB, distilled water, dehydrated in a graded ethanol series, and were coverslipped with mounting medium.

RESULTS

We did not realize that the dog suffered spinal disc herniation. We found the disc herniation when we opened the vertebral lamina and took the spinal cord. The spinal disc herniation revealed at the L3 and S1. Before sacrifice of the dog, the locomotion of the dog seemed no clear dyskinesia when walk the dog. The dog could control excretion and defecation during outdoor walk. We presented example sections of the spinal cord related different segment for the spinal disc herniation as well as the medulla oblongata. The spinal disc herniation located in the ventral of the lumber spinal cord. The compression of the disc herniation caused a signification notch (Figure 1). There was an obvious notch in the ventral of the spinal cord. However, the disc herniation in situ did not cause noticeable neurodegeneration at the level of the notch. Figure 2 caudally located to segment of Figure 1. Vacuolar dendrites of the neurons in vicinity of the central gray matter.

 doi:10.20944/preprints202002.0280.v1

In our previous study, the N-d positive thick neurite termed as megaloneurite is observed in the sacral spinal cord of the aged dog[9]. In the present study, megaloneurites were consistently observed in the dorsal horn of the caudal segments. Figure 3 showed an example of a section that giant megaloneurites occurred in one side dorsal horn while contrast with the same region in the other side. In the Figure 3 B, we pointed out that the megaloneurite (arrowhead) between the lateral collateral pathway [12] [12] and the medial collateral pathway (MCP) could be a new N-d pathway of the autonomic sensory circuit. Temporary, we termed the intermedial collateral pathway with abbreviation ICP. The diameter of the megaloneurite could be as large as 27μm. A tremendous N-d dystrophy and megaloneurites showed in the sacral spinal cord with the notch caused by disc herniation (Figure 4). Besides regular ANBs, we noticed that a massive of N-d spheroids revealed new profile criteria which we termed as homogeneous formazan globule. According to ANBs in aged rat, ANB shows more diversity from size, contour and intensity[13]. The homogeneous formazan globule revealed as round- or oval-shaped non-soma formation and was not found in the normal aged dog[9]. Some of homogeneous formazan globule could also be described like droplet. In this segment, homogeneous formazan globules occurred not only in gray matter but also in the white matter distributed in the dorsal column, lateral funiculus and ventral funiculus. There was also occurrence of the similar variety of neurodystrophy in the intact sacral spinal cord of no herniated compression notch (Figure 5). In the sacral spinal cord distal to the disc herniation, the homogeneous formazan globules greatly reduced (Figure 6). The megaloneurite also reduced. The MCP showed in the figure and indicated the sensory input. The diameter of the megaloneurite also reduced compared with that in Figure 3.

The aging-related N-d neurodegeneration occurred normally in the lumbosacral spinal cord of the aged dog[9, 14]. In the thoracic segment rostral to the disc herniation, no megaloneurite and homogeneous formazan globules were detected besides occasional small size ANBs (Figure 7).

The gracile nucleus receives the primary sensory input bellow the mid thoracic spinal cord[15, 16]. N-d dystrophy corelates to the lumbosacral spinal cord[17] and also occurs in the gracile nucleus of dog[18]. Consideration of the ANBs and the homogeneous formazan globules in the dorsal column, we further examined the gracile nucleus. In Figure 8, ANBs and lightly formazan profiles were detected in the gracile nucleus. Next, ANBs were also detected in the other structures of the medulla, such as in the medial lemniscus (ML), the hypoglossal nucleus (Figure 9) and the ventral lateral of the medulla as well as the spinal trigeminal nucleus (Figure 10). Taken together, the lumen of the central canal regionally collapsed at or near the spinal disc herniation. Away from the disc herniation, the cavity of the central canal was filling around.

DISCUSSION

The case study was completed in a 10-year-old dog accompanied by spinal disc herniation. We have already reported the megaloneurite in the sacral spinal cord of aged dog[9, 14]. In this study, the N-d positive megaloneurite occurred conformally in the sacral spinal cord. We further found that numerous ANBs and enormous homogeneous formazan globules revealed in the gray matter and dorsal column. The homogeneous formazan globule was a novel type of neuropathological profile according to current morphological criteria. In general, megaloneurite and ANB occurred in the dorsal of the gray matter, for example, dorsal horn, Lissauer's tract, dorsal commissural nucleus and intermediolateral nucleus as well as the mediolateral funiculus. We found that the distribution of homogeneous formazan globules occurred not only in the dorsal of the gray matter but also in the ventral horn. The enormous notch caused by spinal disc herniation located at the mid-rostral lumber segments. We did not find the other N-d neurodegenerative aberrant in the tissue of the mid-rostral lumber segment besides the metamorphoses by the compression of the disc herniation. It seemed that the compression

did not cause compression dependent N-d neurodegeneration in situ segment. However, the severe neuropathological changes majorly occurred in the caudal sacral spinal cord. More occurrence of ANB revealed than that of normal aging changes[9]. We supposed that the compression of disc herniation may cause to spread neuropathology from the dorsal part to the ventral area of spinal cord. We should emphasis that the aging-related changes implicated sacral dependent specific mechanism, because the no substantial N-d injury in situ disc herniation and N-d degeneration occurred in distal to disc herniation. The homogeneous formazan globules featured as decellularized extracellular matrix. In the medulla oblongata, ANBs were revealed in the gracile nucleus, nucleus reticularis lateralis (ventrolateral to spinal trigeminal nucleus) and middle of the spinal trigeminal nucleus. In the other species, the similar irregular profiles of the homogeneous formazan globules are detected in the gracile nucleus of aged rats[17]. In the present study, the homogeneous formazan globules were a relative regular profile of the round and oval shape in the sacral spinal cord. Compared with the normal aging alterations in the sacral spinal cord and or the gracile of rat[13, 17], dog[9] and monkey[10] as well as pigeon[19], the homogeneous formazan globules was a novel neurodegenerative formation.

The degenerated intervertebral disk reveal in the spinal disc herniation [20]. Extruded disk herniation is relevant to cell senescence of disc degeneration[21]. The neuropathology of spinal disc herniation is lack in the aging animals. Rat model of lumber disc herniation are used to investigate of the dorsal root ganglia (DRG) and spinal cord[22-26]. Chronic compression of the DRG ipsilaterally induce upregulation of nNOS neurons within the superficial dorsal horn of spinal cord [27]. Basically, nNOS positivity is corelated with N-d expression in the central nervous system[28, 29]. However, some previous investigations demonstrate that N-d is not completely identical to nNOS [13, 30-32]. In our previous study, megaloneurite still identified by the nNOS immunochemistry[14]. Some of N-d dystrophic spheroids in the gracile nucleus also reveal partially colocalization with nNOS immunochemistry[17]. It demonstrates that the N-d neurodegeneration shows diverse properties. Compared with strong stained ANB of sharp boundary, homogeneous formazan globule may be the swollen axons[33] or the deposit of N-d caused by the axonal leakage[34]. ANB is the abbreviation for aging-related N-d body. We thought that the homogeneous formazan globule was compression-related change.

The dystrophic formation in gracile nucleus is aging dependent and has been termed as neuroaxonal dystrophy (NAD)[35-37]. The N-d gracile dystrophy has been reported in the aged rat[36, 38]. We find that N-d neuritic dystrophy occurs in both of the gracile nucleus and cuneatus nucleus of the dorsal column nuclei as well as the spinal trigeminal nucleus[17]. The N-d neuritic dystrophy is pathognomonic morphologic change[17]. In the previous study, the N-d dystrophy is not frequently detected in the aged dog. In the present study, the N-d dystrophy distinctly distributed in the gracile nucleus and several other nuclei.

The medial of dorsal horn of the MCP and the lateral dorsal horn of the LCP are function region for a certain condition [39]. In general anatomy of the thoracolumbar and sacral spinal cord in the dog, N-d positive LCP tracks to the dorsal commissural gray and [40]. In our present study, the megaloneurite in Figure 3 occurrent located lamina III-IV between the LCP and the MCP. The positive labeling of the neuronal tracing of LCP and the dorsal lateral funiculus tracks extending into laminae V-VII in the dorsal commissural gray and vicinity of the parasympathetic nucleus[41]. The immunoactivity of substance P and not VIP distributed in the dorsal horn between the LCP and MCP [42] or no notable evidence demonstrates the confirmation about the fiber connection[43]. In this study, substance P immunoactivity does not show megaloneurite-like profile. Megaloneurite is colocalization with VIP[9, 10]. We thought that the immunoactivity without evidence of projecting fiber may not make a conclusion because the medial portion of the substance P immunoactivity turns to the dorsal commissural region[44]. The two ends of megaloneurite in figure 3 provided clear orientation between the LCP and the MCP. The LCP and MCP are important for urogenital circuit [45] and also for neuropathological condition[46]. The neurons of medial dorsal horn and lateral dorsal horn can be

activated for a physiological function [47]. There was a missing link of notable megaloneurite in the MCP in the Figure 3. Actually, the N-d MCPs were verifiably presented in the Figure 6-1. We also report that megaloneurites locate in the medial dorsal horn of N-d positivity[9] and the VIP positive MCP[14] in aged dog. We postulated that the megaloneurite formed a specific anatomy-oriented functional circuit. As mentioned in results, we already named it a temporary term: intermedial collateral pathway (ICP). We should re-examine the normal spinal cord to verify the neuronal anatomical structure in future.

In summary, the megaloneurite provided a specific anatomy-oriented morphology to reveal a certain circuit in the lumbosacral spinal cord. To our best knowledge, we first time to report the triple morphological alterations of N-d positivity in spinal disc herniation of aged dog. The homogeneous formazan globule was novel neurodegeneration that may implicate the specification of the vulnerable aging deterioration in the sacral spinal cord. We also found that a new circuit pathway: intermedial collateral pathway (ICP) showed by giant megaloneurite between the LCP and the MCP. In the medulla oblongata, ANBs were revealed in the gracile nucleus, nucleus reticularis lateralis (ventrolateral spinal trigeminal nucleus) and middle of the spinal trigeminal nucleus.

ACKNOWLEDGMENTS

This work was supported by grants from National Natural Science Foundation of China (81471286) and Research Start-Up Grant for New Science Faculty of Jinzhou Medical University (173514017).

CONFLICT OF INTERESTS

The authors have no conflicts of interest to declare.

REFERENCES:

[1] A.M. Gorney, S.R. Blau, C.S. Dohse, E.H. Griffith, K.D. Williams, J.H. Lim, D. Knazovicky, B.D. Lascelles, N.J. Olby, Mechanical and Thermal Sensory Testing in Normal Chondrodystrophoid Dogs and Dogs with Spinal Cord Injury caused by Thoracolumbar Intervertebral Disc Herniations, J Vet Intern Med, 30 (2016) 627-635.

[2] C.A. Rousse, N.J. Olby, K. Williams, T.L. Harris, E.H. Griffith, C.L. Mariani, K.R. Munana, P.J. Early, Recovery of stepping and coordination in dogs following acute thoracolumbar intervertebral disc herniations, Vet J, 213 (2016) 59-63.

[3] N.J. Olby, K.R. Müntana, N.J.H. Sharp, D.E. Thrall, THE COMPUTED TOMOGRAPHIC APPEARANCE OF ACUTE THORACOLUMBAR INTERVERTEBRAL DISC HERNIATIONS IN DOGS, Veterinary Radiology & Ultrasound, 41 (2000) 396-402.

[4] N. Olby, E. Griffith, J.M. Levine, Comparison of Gait Assessment Scales in Dogs with Spinal Cord Injury due to Intervertebral Disc Herniation, J Neurotrauma, DOI 10.1089/neu.2019.6804(2020).

[5] H. Itoh, Y. Hara, N. Yoshimi, Y. Harada, Y. Nezu, T. Yogo, H. Ochi, D. Hasegawa, H. Orima, M. Tagawa, A Retrospective Study of Intervertebral Disc Herniation in Dogs in Japan: 297 Cases, Journal of Veterinary Medical Science, 70 (2008) 701-706.

[6] A. Roerig, R. Carlson, A. Tipold, V.M. Stein, Cerebrospinal fluid tau protein as a biomarker for severity of spinal

cord injury in dogs with intervertebral disc herniation, The Veterinary Journal, 197 (2013) 253-258.
[7] J. DUVAL, C. DEWEY, R. ROBERTS, D. ARON, Spinal Cord Swelling as a Myelographic Indicator of Prognosis: A Retrospective Study in Dogs With Intervertebral Disc Disease and Loss of Deep Pain Perception, Veterinary Surgery, 25 (1996) 6-12.
[8] J.-H. Lim, C.-S. Jung, Y.-E. Byeon, W.H. Kim, J.-H. Yoon, K.-S. Kang, O.-k. Kweon, Establishment of a canine spinal cord injury model induced by epidural balloon compression, J Vet Sci, 8 (2007) 89-94.
[9] Y. Li, Y. Jia, W. Hou, Z. Wei, X. Wen, Y. Tian, W. Zhang, L. Bai, A. Guo, G. Du, H. Tan, De novo aging-related megaloneurites: alteration of NADPH diaphorase positivity in the sacral spinal cord of the aged dog, bioRxiv, DOI 10.1101/483990(2019) 483990.
[10] Y. Li, Z. Wei, Y. Jia, W. Hou, Y. Wang, S. Yu, G. Shi, G. Du, H. Tan, Dual forms of aging-related NADPH diaphorase neurodegeneration in the sacral spinal cord of aged non-human primates, bioRxiv, DOI 10.1101/527358(2019) 527358.
[11] T. Nakajima, M. Sakaue, M. Kato, S. Saito, K. Ogawa, K. Taniguchi, Immunohistochemical and enzyme-histochemical study on the accessory olfactory bulb of the dog, The Anatomical record, 252 (1998) 393-402.
[12] M. Tieland, R. Franssen, C. Dullemeijer, C. van Dronkelaar, H. Kyung Kim, T. Ispoglou, K. Zhu, R.L. Prince, L.J.C. van Loon, L. de Groot, The Impact of Dietary Protein or Amino Acid Supplementation on Muscle Mass and Strength in Elderly People: Individual Participant Data and Meta-Analysis of RCT's, The journal of nutrition, health & aging, 21 (2017) 994-1001.
[13] H. Tan, J. He, S. Wang, K. Hirata, Z. Yang, A. Kuraoka, M. Kawabuchi, Age-related NADPH-diaphorase positive bodies in the lumbosacral spinal cord of aged rats, Archives of histology and cytology, 69 (2006) 297-310.
[14] Y. Li, W. Hou, Y. Jia, C. Rao, Z. Wei, X. Xu, H. Li, F. Li, X. Wang, T. Zhang, J. Sun, H. Tan, Megaloneurite, a giant neurite of vasoactive intestinal peptide and nitric oxide synthase in the aged dog and identification by human sacral spinal cord, bioRxiv, DOI 10.1101/726893(2019) 726893.
[15] W.D. Willis, E.D. Al-Chaer, M.J. Quast, K.N. Westlund, A visceral pain pathway in the dorsal column of the spinal cord, Proceedings of the National Academy of Sciences of the United States of America, 96 (1999) 7675-7679.
[16] H.X. Qi, J.H. Kaas, Organization of primary afferent projections to the gracile nucleus of the dorsal column system of primates, The Journal of comparative neurology, 499 (2006) 183-217.
[17] W. Hou, Y. Jia, Y. Li, Z. Wei, X. Wen, C. Rao, X. Xu, F. Li, X. Wu, H. Sun, H. Li, Y. Huang, J. Sun, G. Shu, X. Wang, T. Zhang, G. Shi, A. Guo, S. Xu, G. Du, H. Tan, NADPH diaphorase neuronal dystrophy in gracile nucleus, cuneatus nucleus and spinal trigeminal nucleus in aged rat, bioRxiv, DOI 10.1101/2019.12.21.885988(2019) 2019.2012.2021.885988.
[18] Y. Suzuki, S. Suu, Spheroids (axonal dystrophy) in the central nervous system of the dog, 1: Light microscopic observations, Japanese Journal of Veterinary Science, DOI (1978).
[19] Y. Jia, W. Hou, Y. Li, X. Wen, C. Rao, Z. Wei, T. Zhang, X. Wang, X. Li, L. bai, W. Zhang, P. Wang, J. Bi, A. Guo, J. Wang, H. Tan, A comparative assessment of aging-related NADPH diaphorase positivity in the spinal cord and medullary oblongata between pigeon and murine, bioRxiv, DOI 10.1101/650457(2019) 650457.
[20] M.T. Modic, J.S. Ross, Lumbar degenerative disk disease, Radiology, 245 (2007) 43-61.
[21] S. Roberts, E.H. Evans, D. Kletsas, D.C. Jaffray, S.M. Eisenstein, Senescence in human intervertebral discs, European Spine Journal, 15 (2006) 312-316.
[22] X. Zhu, S. Cao, M.-D. Zhu, J.-Q. Liu, J.-J. Chen, Y.-J. Gao, Contribution of Chemokine CCL2/CCR2 Signaling in the Dorsal Root Ganglion and Spinal Cord to the Maintenance of Neuropathic Pain in a Rat Model of Lumbar Disc Herniation, The Journal of Pain, 15 (2014) 516-526.
[23] T. Ito, S. Ohtori, G. Inoue, T. Koshi, H. Doya, T. Ozawa, T. Saito, H. Moriya, K. Takahashi, Glial Phosphorylated p38 MAP Kinase Mediates Pain in a Rat Model of Lumbar Disc Herniation and Induces Motor Dysfunction in a Rat Model of Lumbar Spinal Canal Stenosis, Spine, 32 (2007) 159-167.
[24] K. Obata, H. Tsujino, H. Yamanaka, D. Yi, T. Fukuoka, N. Hashimoto, K. Yonenobu, H. Yoshikawa, K. Noguchi, Expression of neurotrophic factors in the dorsal root ganglion in a rat model of lumbar disc herniation, Pain, 99 (2002) 121-132.

[25] H.-W. Park, S.-H. Ahn, S.-J. Kim, J.-M. Seo, Y.-W. Cho, S.-H. Jang, S.-J. Hwang, S.-Y. Kwak, Changes in Spinal Cord Expression of Fractalkine and its Receptor in a Rat Model of Disc Herniation by Autologous Nucleus Pulposus, Spine, 36 (2011) E753-E760.

[26] M. Miyagi, T. Ishikawa, S. Orita, Y. Eguchi, H. Kamoda, G. Arai, M. Suzuki, G. Inoue, Y. Aoki, T. Toyone, K. Takahashi, S. Ohtori, Disk Injury in Rats Produces Persistent Increases in Pain-Related Neuropeptides in Dorsal Root Ganglia and Spinal Cord Glia but Only Transient Increases in Inflammatory Mediators: Pathomechanism of Chronic Diskogenic Low Back Pain, Spine, 36 (2011) 2260-2266.

[27] Z.-L. Ma, W. Zhang, X.-P. Gu, W.-S. Yang, Y.-M. Zeng, Effects of intrathecal injection of prednisolone acetate on expression of NR2B subunit and nNOS in spinal cord of rats after chronic compression of dorsal root ganglia, Annals of Clinical & Laboratory Science, 37 (2007) 349-355.

[28] T.M. Dawson, D.S. Bredt, M. Fotuhi, P.M. Hwang, S.H. Snyder, Nitric oxide synthase and neuronal NADPH diaphorase are identical in brain and peripheral tissues, Proceedings of the National Academy of Sciences of the United States of America, 88 (1991) 7797-7801.

[29] B.T. Hope, G.J. Michael, K.M. Knigge, S.R. Vincent, Neuronal NADPH diaphorase is a nitric oxide synthase, Proceedings of the National Academy of Sciences of the United States of America, 88 (1991) 2811-2814.

[30] R.J. Traub, A. Solodkin, S.T. Meller, G.F. Gebhart, Spinal cord NADPH-diaphorase histochemical staining but not nitric oxide synthase immunoreactivity increases following carrageenan-produced hindpaw inflammation in the rat, Brain Res, 668 (1994) 204-210.

[31] A.H. Pullen, P. Humphreys, Diversity in localisation of nitric oxide synthase antigen and NADPH-diaphorase histochemical staining in sacral somatic motor neurones of the cat, Neuroscience letters, 196 (1995) 33-36.

[32] A. Belai, H.H. Schmidt, C.H. Hoyle, C.J. Hassall, M.J. Saffrey, J. Moss, U. Forstermann, F. Murad, G. Burnstock, Colocalization of nitric oxide synthase and NADPH-diaphorase in the myenteric plexus of the rat gut, Neuroscience letters, 143 (1992) 60-64.

[33] F.A. ZAKI, Odontoid process dysplasia in a dog, Journal of Small Animal Practice, 21 (1980) 227-234.

[34] A.-W. Xiao, J. He, Q. Wang, Y. Luo, Y. Sun, Y.-P. Zhou, Y. Guan, P.J. Lucassen, J.-P. Dai, The origin and development of plaques and phosphorylated tau are associated with axonopathy in Alzheimer's disease, Neuroscience bulletin, 27 (2011) 287.

[35] F. Seitelberger, Neuropathological conditions related to neuroaxonal dystrophy, Symposium on Pathology of Axons and Axonal Flow, Springer, 1971, pp. 17-29.

[36] S. Ma, M.E. Cornford, I. Vahabnezhad, S. Wei, X. Li, Responses of nitric oxide synthase expression in the gracile nucleus to sciatic nerve injury in young and aged rats, Brain Res, 855 (2000) 124-131.

[37] K. Jellinger, A. Jirásek, Neuroaxonal dystrophy in man: character and natural history, Symposium on Pathology of Axons and Axonal Flow, Springer, 1971, pp. 3-16.

[38] S.X. Ma, A.T. Holley, A. Sandra, M.D. Cassell, F.M. Abboud, Increased expression of nitric oxide synthase in the gracile nucleus of aged rats, Neuroscience, 76 (1997) 659-663.

[39] P. Zvara, M.A. Vizzard, Exogenous overexpression of nerve growth factor in the urinary bladder produces bladder overactivity and altered micturition circuitry in the lumbosacral spinal cord, BMC physiology, 7 (2007) 9.

[40] M.A. Vizzard, K. Erickson, W.C. de Groat, Localization of NADPH diaphorase in the thoracolumbar and sacrococcygeal spinal cord of the dog, Journal of the autonomic nervous system, 64 (1997) 128-142.

[41] W.D. Steers, J. Ciambotti, B. Etzel, S. Erdman, W.C. de Groat, Alterations in afferent pathways from the urinary bladder of the rat in response to partial urethral obstruction, Journal of Comparative Neurology, 310 (1991) 401-410.

[42] M. Kawatani, I. Lowe, I. Nadelhaft, C. Morgan, W.C. De Groat, Vasoactive intestinal polypeptide in visceral afferent pathways to the sacral spinal cord of the cat, Neuroscience letters, 42 (1983) 311-316.

[43] W.C. de Groat, M. Kawatani, T. Hisamitsu, I. Lowe, C. Morgan, J. Roppolo, A.M. Booth, I. Nadelhaft, D. Kuo, K. Thor, The role of neuropeptides in the sacral autonomic reflex pathways of the cat, Journal of the autonomic nervous system, 7 (1983) 339-350.

[44] M. Kawatani, S.L. Erdman, W.C. de Groat, Vasoactive intestinal polypeptide and substance P in primary afferent

 doi:10.20944/preprints202002.0280.v1

pathways to the sacral spinal cord of the cat, The Journal of comparative neurology, 241 (1985) 327-347.
[45] R.E. Papka, J. Hafemeister, B.A. Puder, S. Usip, M. Storey-Workley, Estrogen receptor-α and neural circuits to the spinal cord during pregnancy, Journal of Neuroscience Research, 70 (2002) 808-816.
[46] V.G. VanderHorst, T. Samardzic, C.B. Saper, M.P. Anderson, S. Nag, J.A. Schneider, D.A. Bennett, A.S. Buchman, alpha-Synuclein pathology accumulates in sacral spinal visceral sensory pathways, Annals of neurology, 78 (2015) 142-149.
[47] B.A. Puder, R.E. Papka, Activation and circuitry of uterine-cervix-related neurons in the lumbosacral dorsal root ganglia and spinal cord at parturition, Journal of Neuroscience Research, 82 (2005) 875-889.

Preprints (www.preprints.org) | NOT PEER-REVIEWED | Posted: 19 February 2020 doi:10.20944/preprints202002.0280.v1

FIGURE LEGENDS:

Figure 1. Montaged image of the coronal transverse section at the spinal disc herniation. Arrow indicated neuron. Open arrow: slightly stained motoneuron. Arrowhead: enlarged transverse fiber. Open arrowhead: fiber.

Figure 2. Vacuolar dendrites in the lumber spinal cord of caudal to the spinal disc herniation. A-E showed vacuolar dendrites with serial magnifications in C-D from the same field A. F showed thick dendrite of diverse staining. Bar in A =200μm, B- =100μm, C= 50μm, and D-F and inset =20μm.

Figure 3. Giant megaloneurite in the circuit pathway of the dorsal horn. A: Montaged photography at no noticeable level of the lumber spinal cord. B: The megaloneurite occurred in the pathway of the Lissauer's tract and lateral dorsal horn, lateral collateral pathway, circuit pathway (arrowheads) between the MCP and the LCP. C magnification from small rectangle in A and showed ANBs of strong staining (curved open arrow) and diverse staining (open arrow). D and E showed megaloneurite (arrowhead), neurons (arrow) and thin fiber (open arrowhead). F and G showed the same location of the left and right side of the LCP (circle double arrow). Three size diameter fibers: megaloneurite (F), thick fiber (arrowhead) and thin fiber (open arrowhead). Bar in A = 200μm, B =100 μm, C, E, F and G =20μm, and D =50μm.

Figure 4-1. Diverse N-d dystrophy and megaloneurite cross the dorsal commissural gray in the sacral spinal cord. The notches (large open arrow) were corelated disc herniation. Some neuro-dystrophic spheroids distributed in the white matter around the anterior horn. Arrow indicated a neuron. Arrowhead indicated the megaloneurite. Open arrow indicated homogeneous formazan globule. Thin arrow indicated strong stained ANB in the Lissauer's tract. Curved arrow indicated spheroid in the dorsal column (DC). Curved thin arrow indicated the transverse megaloneurite in the lateral funiculus (LF). cc：central canal. Bar =200μm.

Figure 4-2. A showed megaloneurite (arrowhead). B showed homogeneous formazan globule (open arrow) distributed both in the lateral funiculus (LF) and the gray matter. Dash line indicated boundary. C showed dystrophy (curved arrow) between the ependymal cells. D: magnification from C showed various fibers and megaloneurite as well as homogeneous formazan globule (open arrow). D further showed ANB (curved arrow), megaloneurite (circle double arrows), an example of thin fiber (open arrowhead). Bar in A =100μm, B, D and E =20μm, C = 50μm.

Figure 4-3. A: The distribution of N-d dystrophy including homogeneous formazan globules in the dorsal lateral region. B-E were magnification from A. B: The megaloneurites and their segments distributed in the Lissauer's tract (LT) and the lateral collateral pathway [12](arrowhead). Magnification in D. Curved thin arrow indicated an example of transverse megaloneurite. E showed transverse megaloneurite (curved thin arrow) in the lateral funiculus (LF). F showed the other side of the LT. Bar in A =100μm, B, C and E =50μm, D and F = 20μm.

Figure 5. The sacral spinal cord of no herniated notch. A: no disc herniation notch. Insets showed the transverse thick fiber in the lateral funiculus, megaloneurites in the Lissauer's tract and neurons in the anterior horn respectively. B showed various N-d passivity of homogeneous formazan globules (open arrow), megaloneurite (arrowhead), thin fiber (open arrowhead) and irregular ANB. Bar in A =200μm, bar in inset and B =50μm.

Figure 6-1. The MCP in the sacral spinal cord caudal to Figure 5.A-E showed the MCP. Arrow: neuron, arrowhead： megaloneurite in the MCP. Open arrowhead: thin fiber in the MCP and curved open arrow: ANB. White litter for Figure 6-2. Bar in A=200μm, B= 100μm, C=50μm, D and F = 20μm.

Preprints (www.preprints.org) | NOT PEER-REVIEWED | Posted: 19 February 2020 doi:10.20944/preprints202002.0280.v1

Figure 6-2. Present the white letters in Figure 6-1A. Bar =50μm.

Figure 7. The intact thoracic spinal cord. A: The transverse spinal cord of no herniated notch. B: No megaloneurite and homogeneous formazan globules. C and D showed the intermediolateral nucleus (IML). Inset showed ANBs. Arrow indicated neurons. E: Magnification from D. F: showed the anterior horn and motoneurons (arrow). Bar in A = 200μm, B= 100μm, C, D and F =50μm and E =20μm.

Figure 8. ANB and lightly formazan profile detected in the gracile nucleus. All figure showed here from the same section. A: low magnification view of the gracile nucleus. B: magnification from A. Arrow indicated neuron consistent in I. C: Several ANBs showed. Arrowhead indicated strong stained ANB. Thin arrow indicated fibers. Open arrowhead indicated. D: Lightly stained ANB and strong stained Two rectangles (E and F). E showed weak N-d spheroid (open arrow) and N-d positivity of blurred boundary(asterisk). F showed ANBs compared small size spheroids (open arrowhead) with fibers (thin arrow). G showed cloudy prion-like staining and puncta (open arrowhead) compared with fibers (thin arrow). H and I showed similar examples of neuro-dystrophy. Curved open arrow indicated a vacuolar neuro-dystrophy (H). Arrow indicated a neuron (I). Bar in A = 200μm, B =100μm, C, G, H and I =20μm, D, E and F = 50μm.

Figure 9. ANB detected in the other structures of the medulla. A and B indicated ANBs (open arrow) in the medial lemniscus (ML). C and D showed swelling (arrowhead) in the root of nerve XII (asterisk). Arrow indicated a multiple neuron with thick vacuolized proximal dendrites. E and F showed cloudy neuro-dystrophy in the hypoglossal nucleus (dash line). Bar in A, C and E =100μm. Bar in B, D and F =20μm.

Figure 10. ANB detected in the other structures of the medulla. A, B and C showed ANBs in the ventral lateral of the medulla. Open arrows in B indicated ANBs. D, E and F showed the ANBs in the spinal trigeminal nucleus. Bar in A and D = 200μm, in B and E 100μm and in C and F = 20μm.

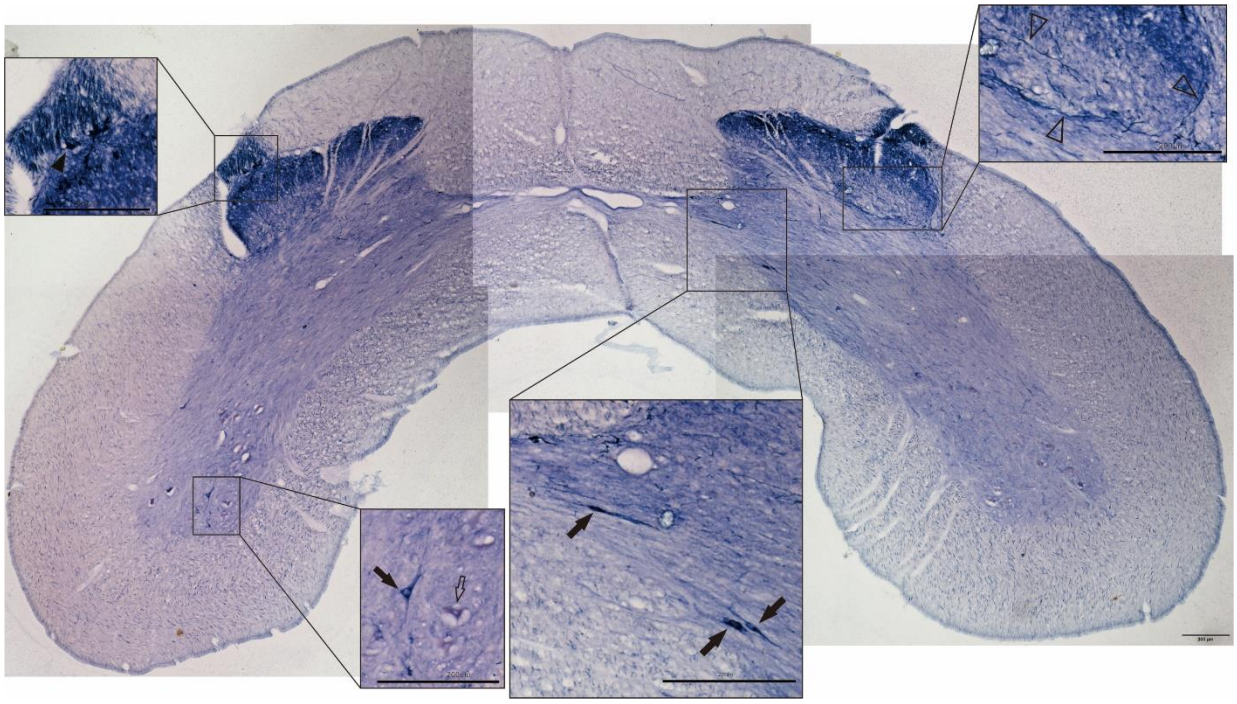

Figure 1. Montaged photograph of the coronal transverse section at the level of spinal disc herniation. The compression of the disc herniation caused a big notch ventral to the anterior median fissure. Arrow indicated neuron. Open arrow: slightly stained motoneuron. Arrowhead: enlarged transverse fiber. Open arrowhead: fiber. Bar =200μm.

Preprints (www.preprints.org) | NOT PEER-REVIEWED | Posted: 19 February 2020 doi:10.20944/preprints202002.0280.v1

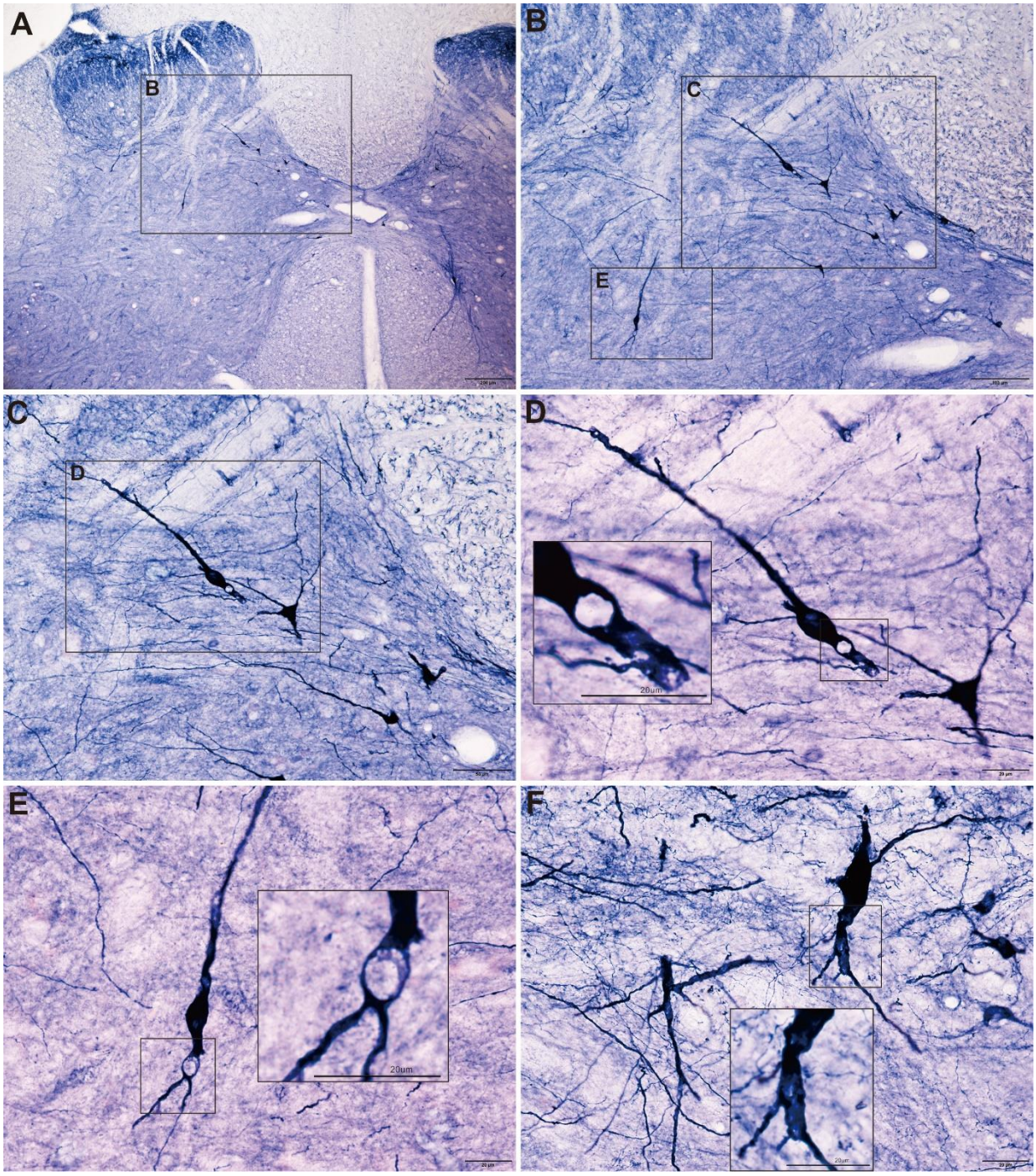

Figure 2. Vacuolar dendrites in the lumber spinal cord of caudal to the spinal disc herniation. A-E showed vacuolar dendrites with serial magnifications in C-D from the same field A. F showed thick dendrite of diverse staining. Bar in A =200μm, B- =100μm, C= 50μm, and D-F and inset =20μm.

Preprints (www.preprints.org) | NOT PEER-REVIEWED | Posted: 19 February 2020 doi:10.20944/preprints202002.0280.v1

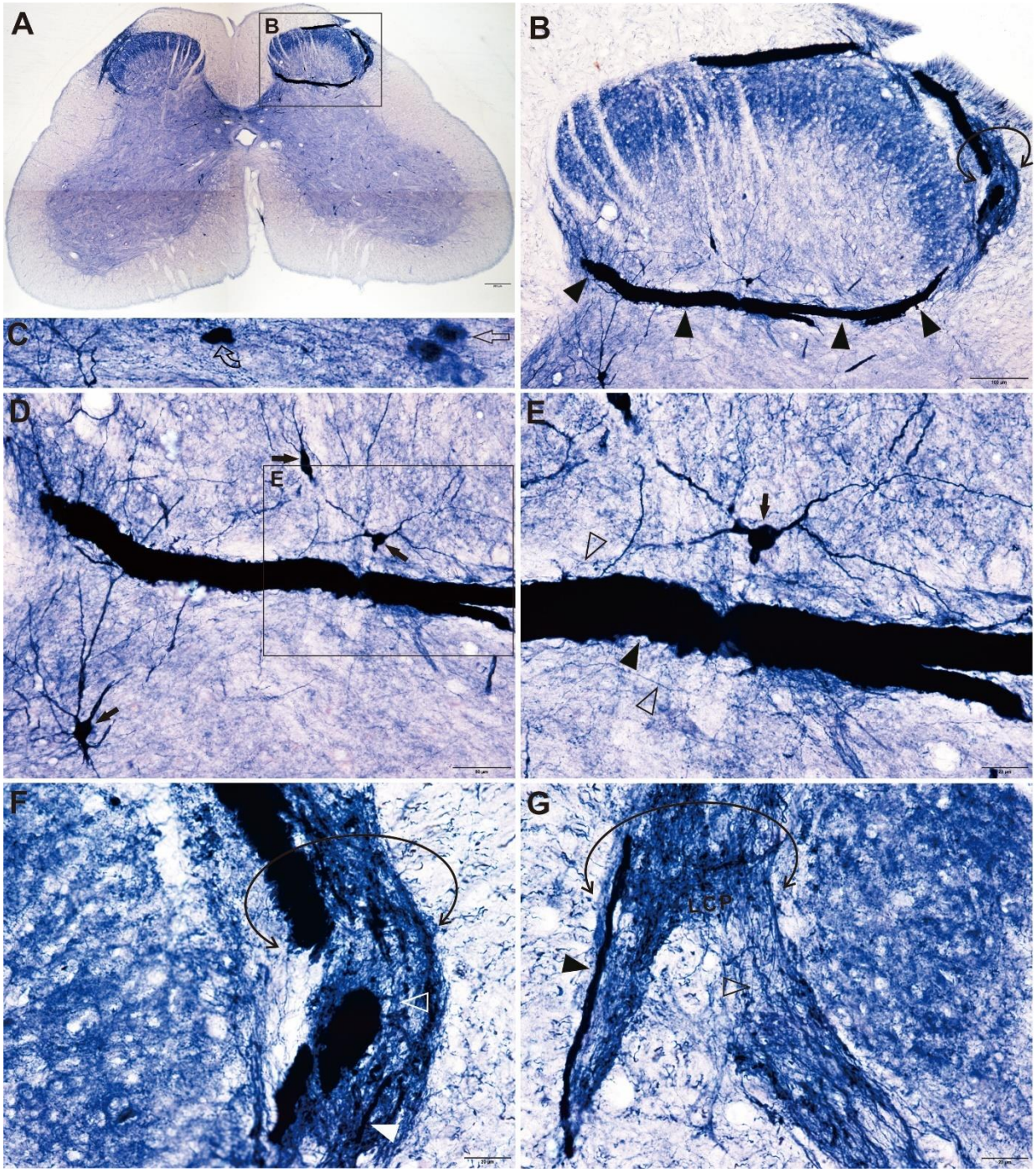

Figure 3. Giant megaloneurite in the circuit pathway of the dorsal horn. A: Montaged photography at no noticeable level of the lumber spinal cord. B: The megaloneurite occurred in the pathway of the Lissauer's tract and lateral dorsal horn, lateral collateral pathway, circuit pathway (arrowheads) between the MCP and the LCP. C magnification from small rectangle in A and showed ANBs of strong staining (curved open arrow) and diverse staining (open arrow). D and E showed megaloneurite (arrowhead), neurons (arrow) and thin fiber (open arrowhead). F and G showed the same location of the left and right side of the LCP (circle double arrow). Three size diameter fibers: megaloneurite (F), thick fiber (arrowhead) and thin fiber (open arrowhead). Bar in A = 200μm, B =100μm, C, E, F and G =20μm, and D =50μm.

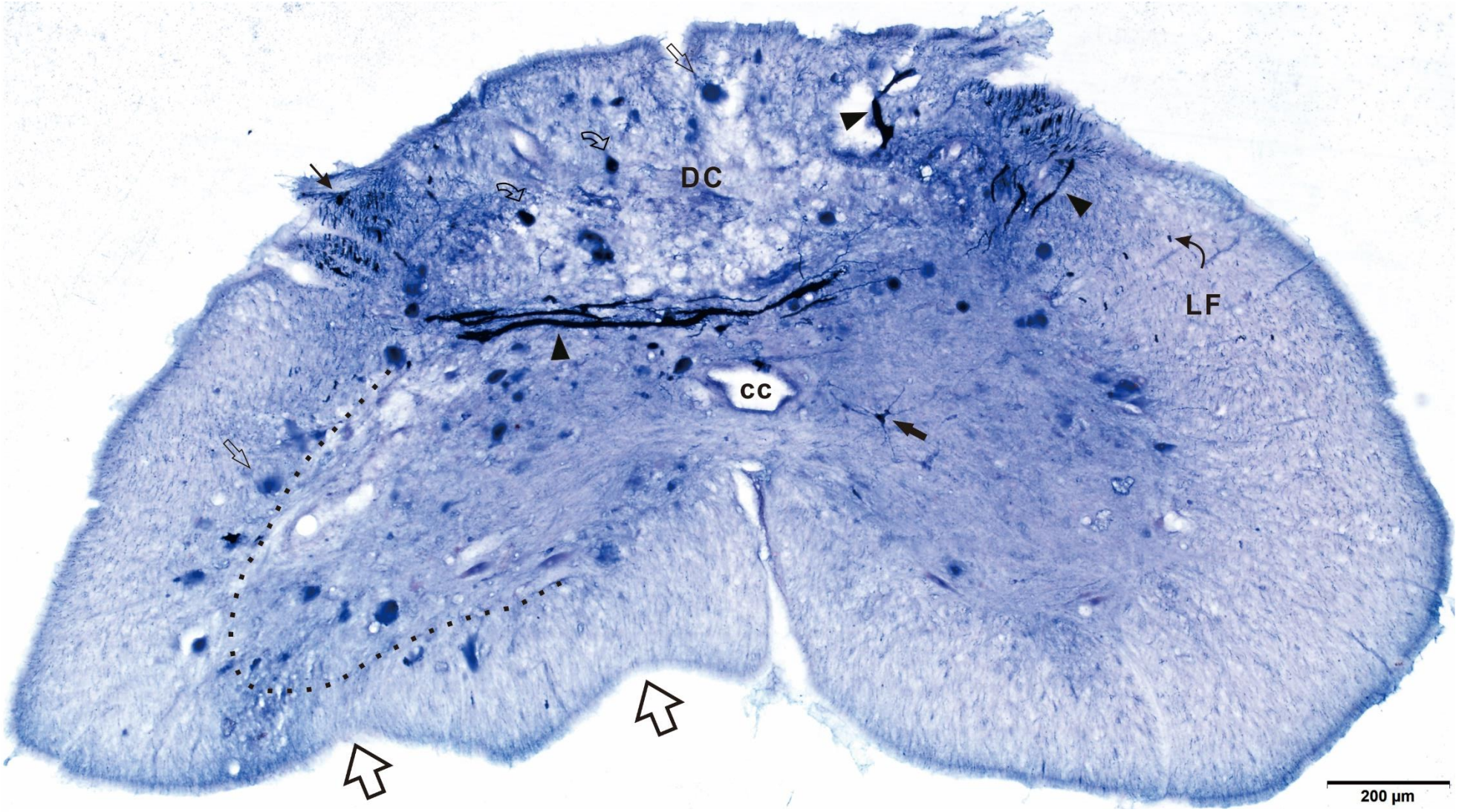

Figure 4-1. Diverse N-d dystrophy and megaloneurite cross the dorsal commissural gray in the sacral spinal cord. The notches (large open arrow) were corelated disc herniation. Some neuro-dystrophic spheroids distributed in the white matter around the anterior horn. Arrow indicated a neuron. Arrowhead indicated the megaloneurite. Open arrow indicated homogeneous formazan globule. Thin arrow indicated strong stained ANB in the Lissauer's tract. Curved arrow indicated spheroid in the dorsal column (DC). Curved thin arrow indicated the transverse megaloneurite in the lateral funiculus (LF). cc: central canal. Bar =200μm.

doi:10.20944/preprints202002.0280.v1

Preprints (www.preprints.org) | NOT PEER-REVIEWED | Posted: 19 February 2020 doi:10.20944/preprints202002.0280.v1

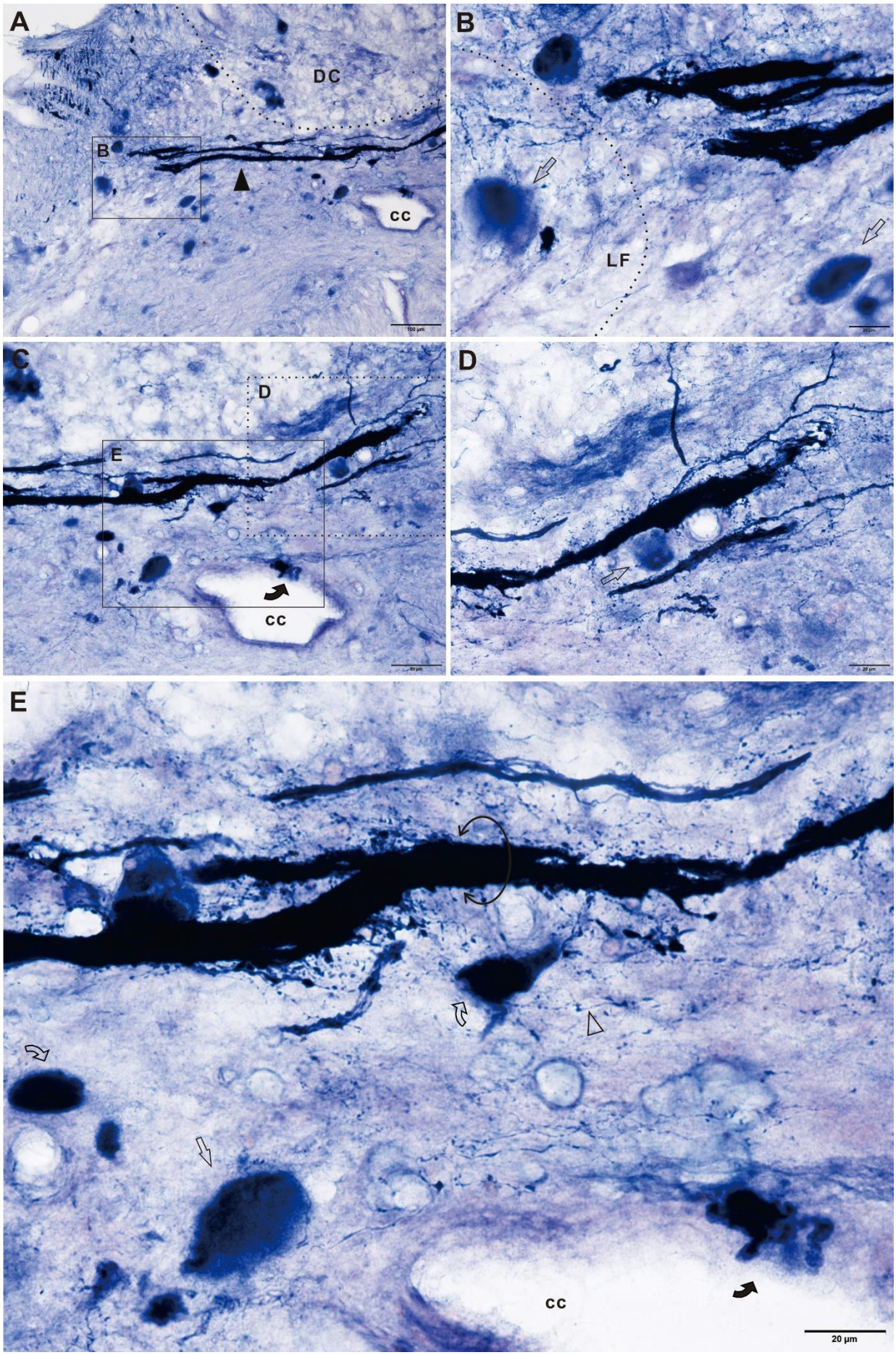

Figure 4-2. A showed megaloneurite (arrowhead). B showed homogeneous formazan globule (open arrow) distributed both in the lateral funiculus (LF) and the gray matter. Dash line indicated boundary. C showed dystrophy (curved arrow) between the ependymal cells. D: magnification from C showed various fibers and

Preprints (www.preprints.org) | NOT PEER-REVIEWED | Posted: 19 February 2020 doi:10.20944/preprints202002.0280.v1

megaloneurite as well as homogeneous formazan globule (open arrow). D further showed ANB (curved arrow), megaloneurite (circle double arrows), an example of thin fiber (open arrowhead). Bar in A =100μm, B, D and E =20μm, C = 50μm.

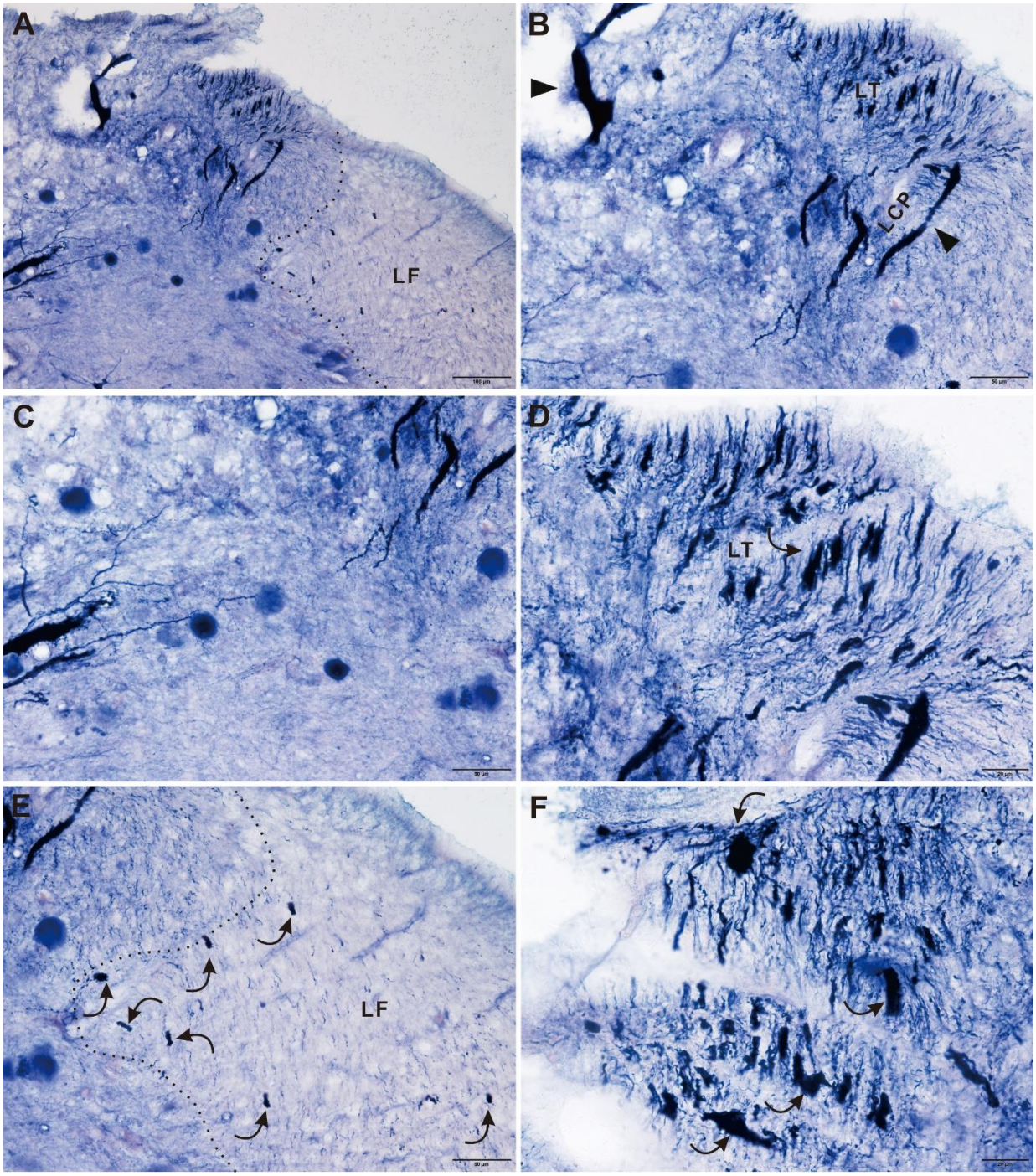

Figure 4-3. A: The distribution of N-d dystrophy including homogeneous formazan globules in the dorsal lateral region. B-E were magnification from A. B: The megaloneurites and their segments distributed in the Lissauer's tract (LT) and the lateral collateral pathway [12](arrowhead). Magnification in D. Curved thin arrow indicated an example of transverse megaloneurite. E showed transverse megaloneurite (Curved thin arrow) in the lateral funiculus (LF). F showed the other side of the LT. Bar in A =100μm, B, C and E =50μm, D and F = 20μm.

Preprints (www.preprints.org) | NOT PEER-REVIEWED | Posted: 19 February 2020 doi:10.20944/preprints202002.0280.v1

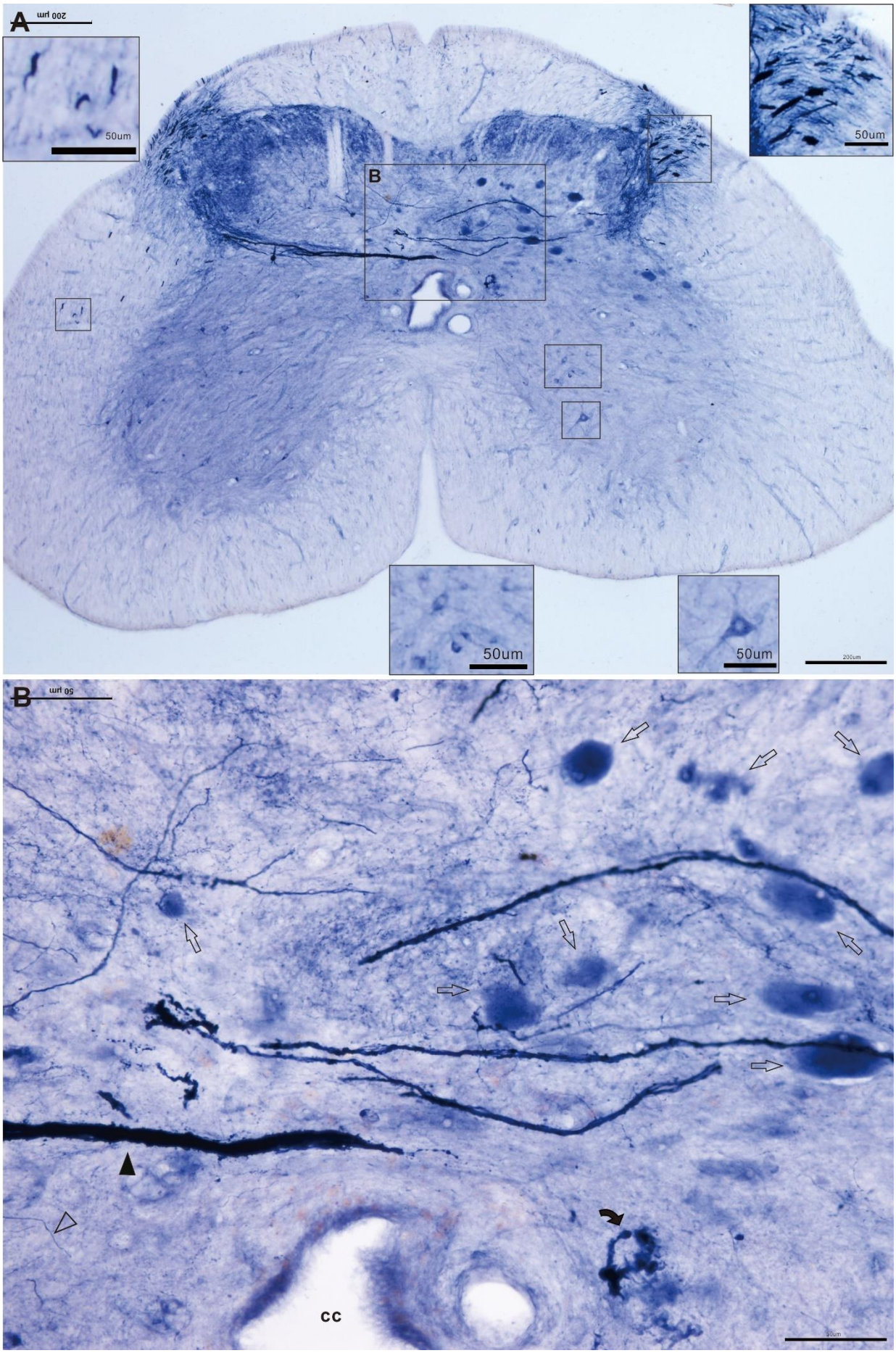

Figure 5. The sacral spinal cord of no herniated notch. A: no disc herniation notch. Insets showed the transverse thick fiber in the lateral funiculus, megaloneurites in the Lissauer's tract and neurons in the anterior horn

Preprints (www.preprints.org) | NOT PEER-REVIEWED | Posted: 19 February 2020 doi:10.20944/preprints202002.0280.v1

respectively. B showed various N-d passivity of homogeneous formazan globules (open arrow), megaloneurite (arrowhead), thin fiber (open arrowhead) and irregular ANB. Bar in A =200μm, bar in inset and B =50μm.

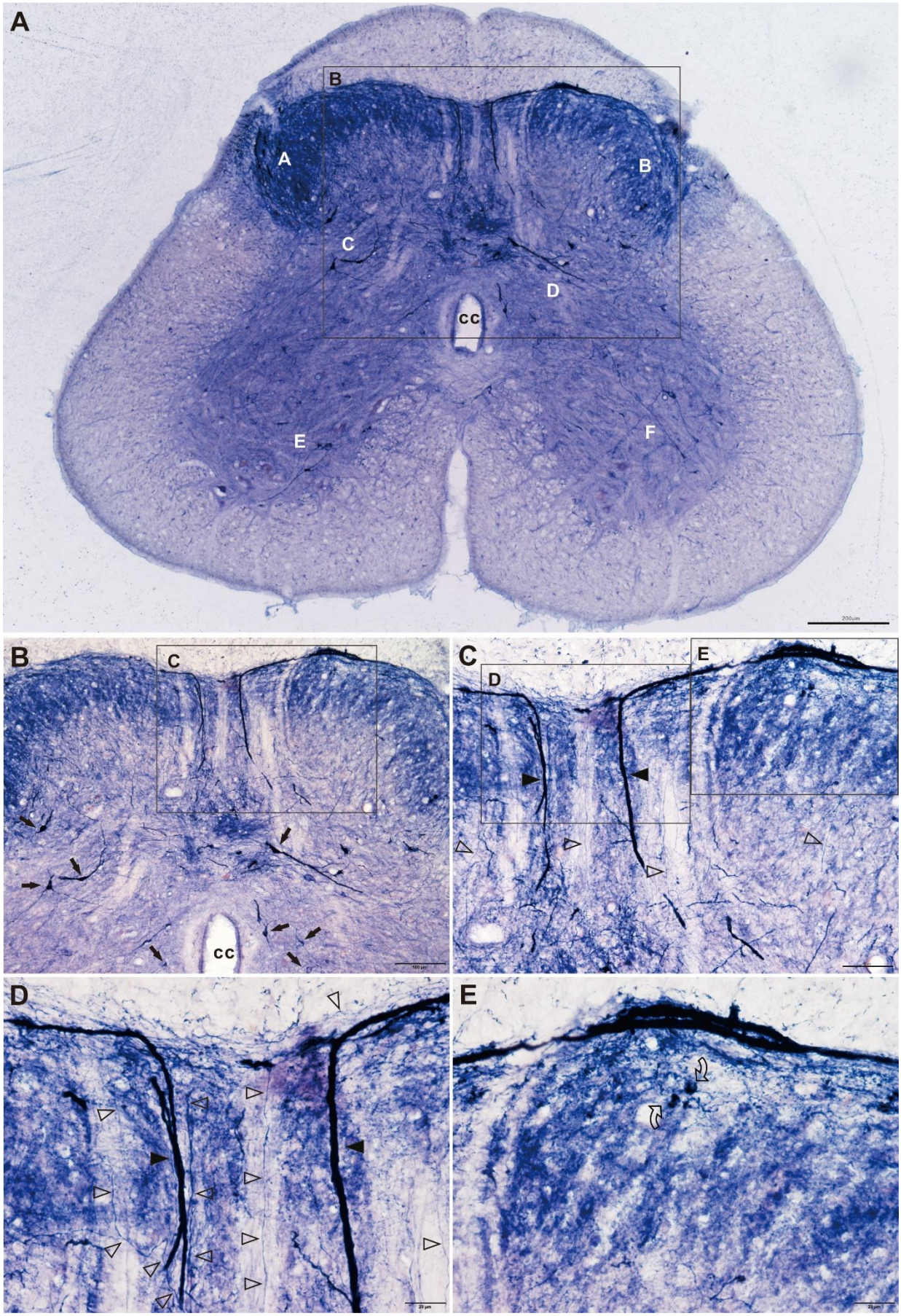

Figure 6-1. The MCP in the sacral spinal cord caudal to Figure 5.A-E showed the MCP. Arrow: neuron,

Preprints (www.preprints.org) | NOT PEER-REVIEWED | Posted: 19 February 2020 doi:10.20944/preprints202002.0280.v1

arrowhead： megaloneurite in the MCP. Open arrowhead: thin fiber in the MCP and curved open arrow: ANB. White litter for Figure 6-2. Bar in A=200μm, B= 100μm, C=50μm, D and F = 20μm.

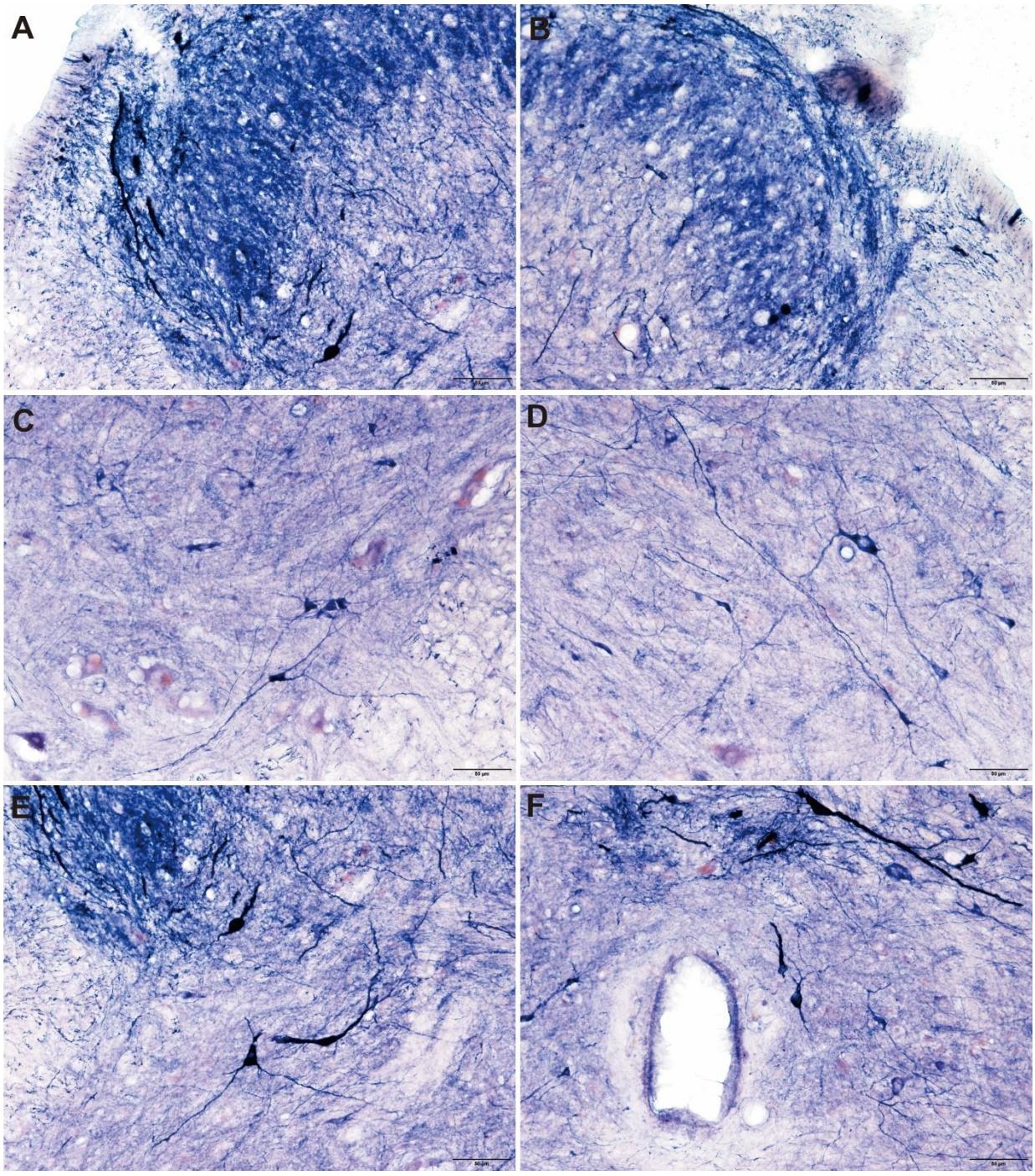

Figure 6-2. Present the white letters in Figure 6-1A. Bar =50μm.

Preprints (www.preprints.org) | NOT PEER-REVIEWED | Posted: 19 February 2020 doi:10.20944/preprints202002.0280.v1

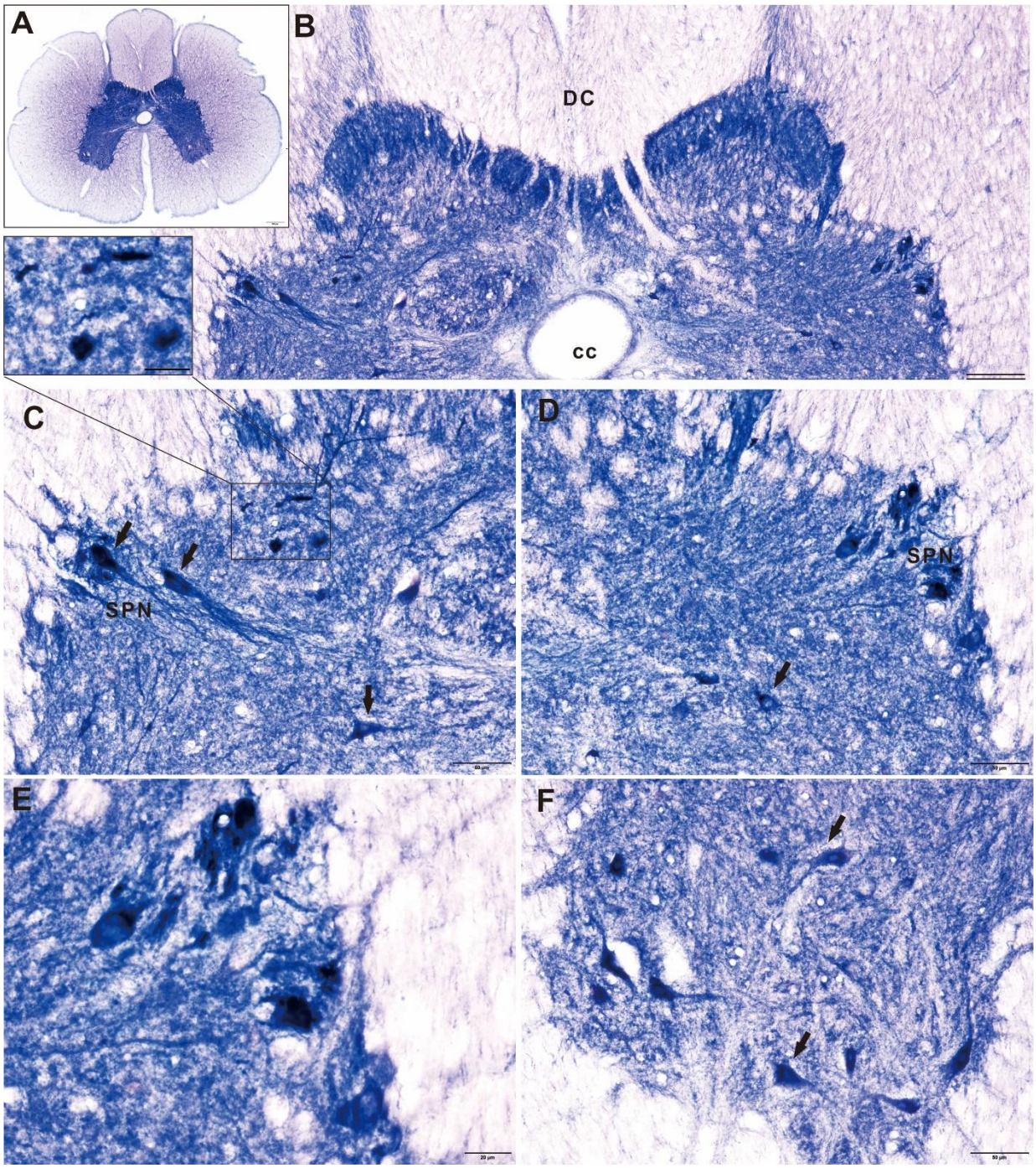

Figure 7. The intact thoracic spinal cord. A: The transverse spinal cord of no herniated notch. B: No megaloneurite and homogeneous formazan globules. C and D showed the intermediolateral nucleus (IML). Inset showed ANBs. Arrow indicated neurons. E: Magnification from D. F: showed the anterior horn and motoneurons (arrow). Bar in A = 200μm, B= 100μm, C, D and F =50μm and E =20μm.

Preprints (www.preprints.org) | NOT PEER-REVIEWED | Posted: 19 February 2020 doi:10.20944/preprints202002.0280.v1

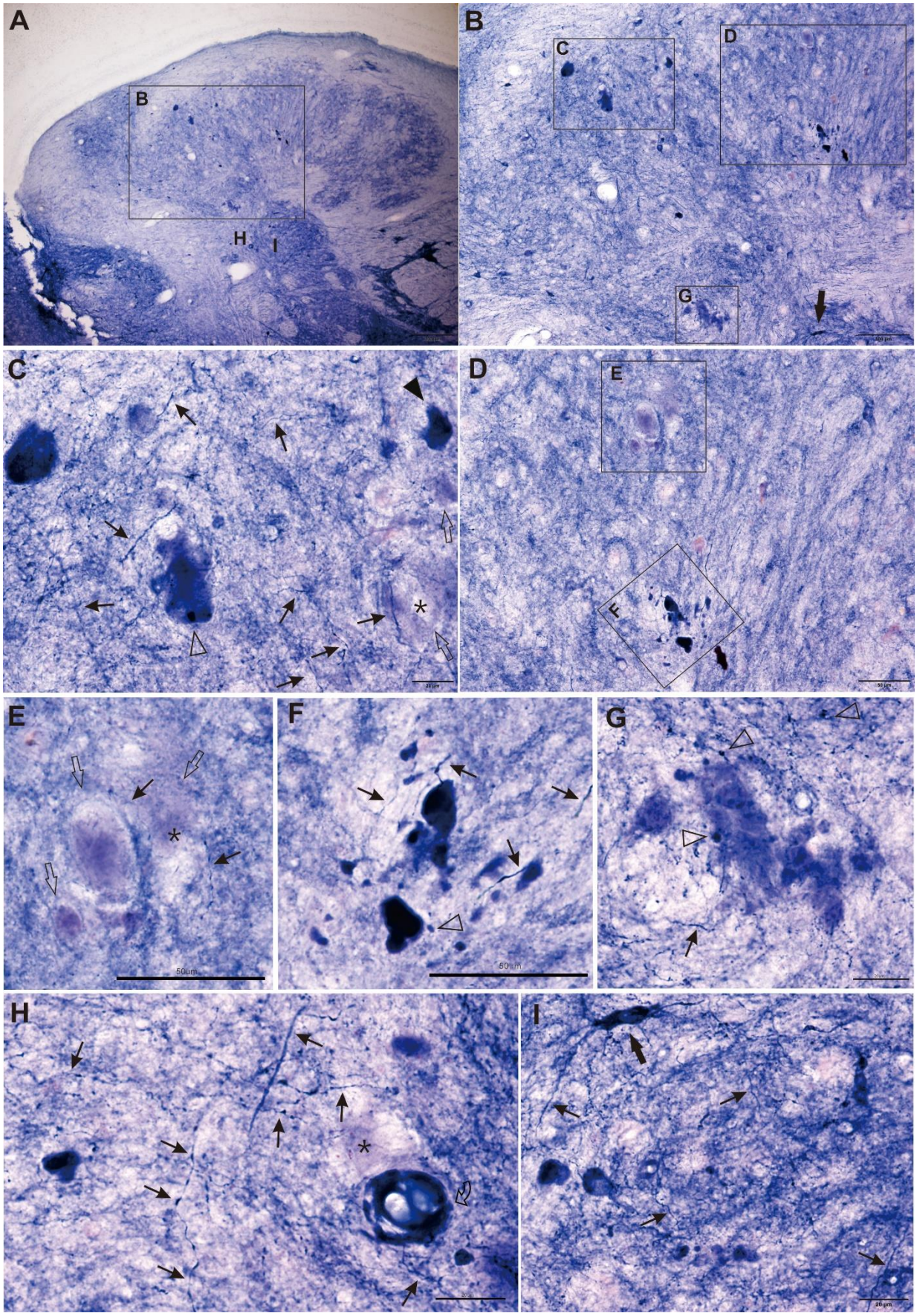

Figure 8. ANB and lightly formazan profile detected in the gracile nucleus. All figure showed here from the same section. A: low magnification view of the gracile nucleus. B: magnification from A. Arrow indicated neuron consistent in I. C: Several ANBs showed. Arrowhead indicated strong stained ANB. Thin arrow indicated fibers. Open arrowhead indicated. D: Lightly stained ANB and strong stained Two rectangles (E and F). E showed weak N-d spheroid (open arrow) and N-d positivity of blurred boundary(asterisk). F showed

Preprints (www.preprints.org) | NOT PEER-REVIEWED | Posted: 19 February 2020 doi:10.20944/preprints202002.0280.v1

ANBs compared small size spheroids (open arrowhead) with fibers (thin arrow). G showed cloudy prion-like staining and puncta (open arrowhead) compared with fibers (thin arrow). H and I showed similar examples of neuro-dystrophy. Curved open arrow indicated a vacuolar neuro-dystrophy (H). Arrow indicated a neuron (I). Bar in A = 200μm, B =100μm, C, G, H and I =20μm, D, E and F = 50μm.

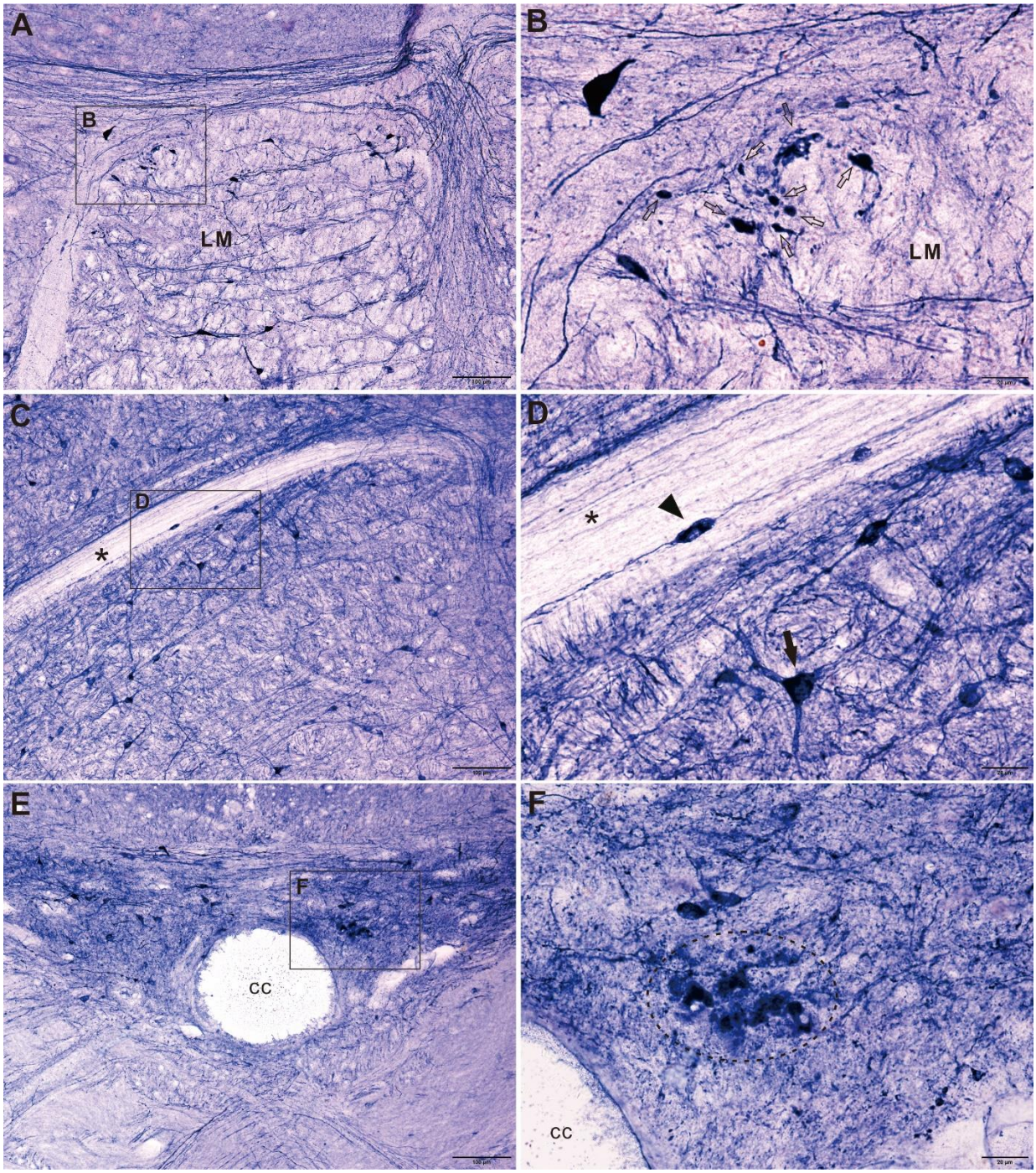

Figure 9. ANB detected in the other structures of the medulla. A and B indicated ANBs (open arrow) in the medial lemniscus (ML). C and D showed swelling (arrowhead) in the root of nerve XII (asterisk). Arrow indicated a multiple neuron with thick vacuolized proximal dendrites. E and F showed cloudy neuro-dystrophy in the hypoglossal nucleus (dash line). Bar in A, C and E =100μm. Bar in B, D and F =20μm.

Preprints (www.preprints.org) | NOT PEER-REVIEWED | Posted: 19 February 2020 doi:10.20944/preprints202002.0280.v1

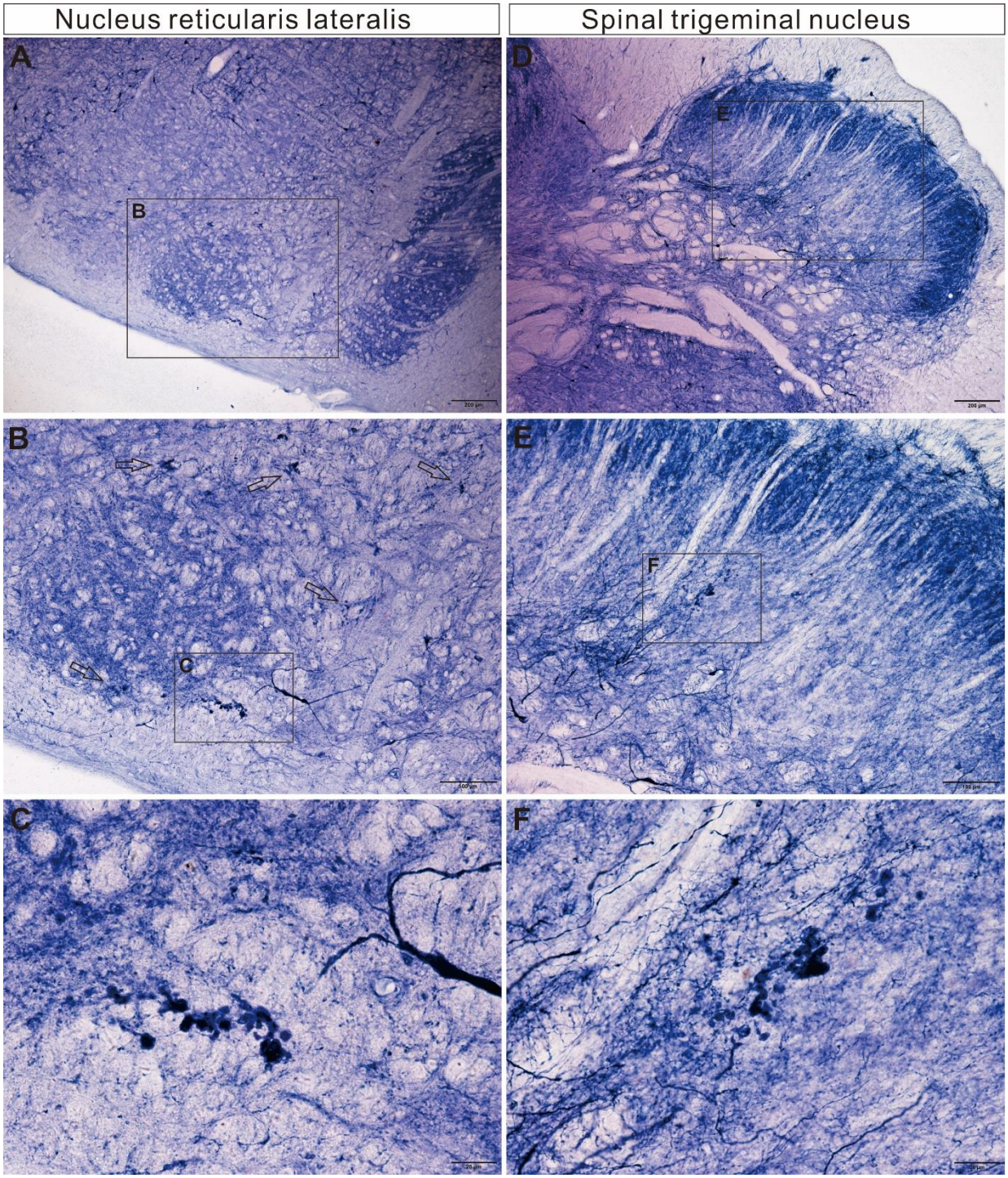

Figure 10. ANB detected in the other structures of the medulla. A, B and C showed ANBs in the ventral lateral of the medulla. Open arrows in B indicated ANBs. D, E and F showed the ANBs in the spinal trigeminal nucleus. Bar in A and D = 200μm, in B and E 100μm and in C and F = 20μm.